


Research

Delineating petrological feature and geochemical characteristics of volcanic rocks from the Herson-Kilkis Area, Northern Greece

Akindynos E. Kelepertsis¹ · Dimitrios E. Alexakis² 

Received: 11 January 2024 / Accepted: 24 May 2024

Published online: 03 June 2024

© The Author(s) 2024 [OPEN](#)

Abstract

The geochemical data of this study confirm a previous suggestion that the Herson—Kilkis rhyolites are the crystallization products of a magma generated by the partial fusion of K-rich schists or para-gneisses and erupted along a dip-slip fault at the western boundary of the Serbo—Macedonian massif. High-K rhyolites occur in the area around Kilkis town along the western boundary of the Serbo-Macedonian massif. The chemistry of the rocks is characterized by high K₂O contents (7–12 Wt %), high K₂O/Na₂O ratios (2–22), low CaO (0.04–0.16%) and Sr (0–83 mg Kg⁻¹) contents and high Rb/Sr ratios (4–40). The trace elements (in mg Kg⁻¹), Nb (Not Detected–41), Nd (5–87), Ce (16–119), La (9–67), Rb (Not Detected–358) and Y (10–87) present higher contents than those of rhyolites derived from a more basic magma by low-pressure fractional crystallization.

Keywords Volcanic rocks · Rhyolites · Herson area · Greece

1 Introduction

The majority of field evidence suggests that igneous rocks are the result of the upward-moving bodies of either magma, mixes of magma and crystals, magma and gas bubbles, or even solid rock [36]. Basaltic lava flows extensively cover the majority of the ocean floor and vast regions of continents. Rhyolitic lava flows and volcanic ash extensively covers vast areas of continents. Magma with diverse compositions can rise to the Earth's surface [36]. Exposures of deeply eroded sections of the Earth's crust demonstrate that basaltic magmas typically ascend through fractures and, upon cooling, create inclined sheet-like intrusions called dikes [36]. Rhyolitic magmas, on the other hand, typically rise in expansive dome-shaped structures called diapirs. When these diapirs solidify beneath the Earth's surface, they form granite batholiths [36]. Rhyolite is frequently found in areas where two tectonic plates are colliding, causing one plate of oceanic lithosphere to sink beneath another plate of oceanic or continental lithosphere into the Earth's mantle. It can occasionally be the most common form of igneous rock in these environments. Rhyolite is more prevalent when the lithosphere on top is continental rather than oceanic. According to Ayalew and Ishiwatari [2], rhyolites occur in many types of tectonic settings, although their proportion ranges greatly from one tectonic setting to another. There are many scientific arguments regarding the origin of rhyolites. In general, the following petrogenetic models have been proposed [2]: (a) fractional

✉ Dimitrios E. Alexakis, d.alexakis@uniwa.gr; Akindynos E. Kelepertsis, kelepertsis@geol.uoa.gr | ¹Faculty of Geology and Geoenvironment, University of Athens, Panepistimiopolis, Zographou, 157 84 Athens, Greece. ²Laboratory of Geoenvironmental Science and Environmental Quality Assurance, Department of Civil Engineering, School of Engineering, University of West Attica, 250 Thivon & P. Ralli Str, 12241 Athens, Greece.

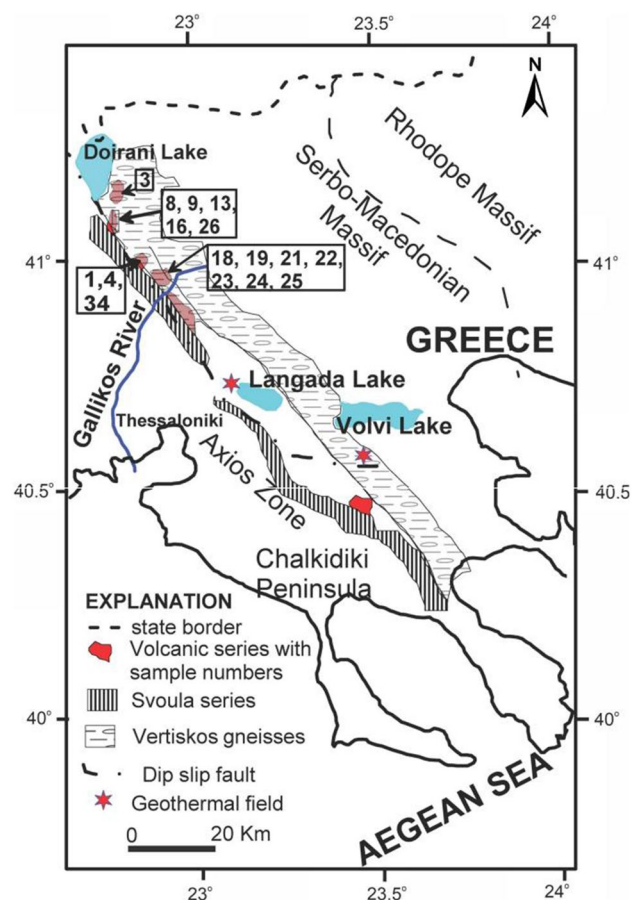


crystallization with or without crustal assimilation or contamination, and (b) partial melting of solidified basalt magma/partial melting of crustal materials.

According to Philpotts and Ague [36], the increased thickness of the continental crust provides greater chances for the rising magma to undergo differentiation and assimilate crustal rock. Rhyolite has been found on remote islands, however, such instances in the ocean are uncommon. Tholeiitic magmas, which are erupted at volcanic ocean islands like Iceland, can undergo complete differentiation and transform into rhyolite [36].

Rhyolites are important stratigraphic markers that provide precise ages and indicate where thermal pulses from the mantle are injected into the crust through basalt injection, regardless of rhyolite petrogenesis details [38]. Along the western boundary of the Serbo-Macedonian massif (Central Macedonia), there are occurrences of volcanic rocks of the so-called "Volcano-sedimentary series" [31]. These rocks are situated in a belt a few km wide and strike NW—SE, parallel to the western boundary of the Serbo-Macedonian massif (Fig. 1). Kelepertsis et al. [18] presented a new understanding of the geology, age and geochemistry of the volcano-sedimentary series near Pyrgoto village, where the rocks are predominantly K_2O -rich quartz trachytes. The series has been assigned to the Strymonikon—Metamorphosis volcanic arc [25, 30]. The volcanic rocks of this arc are encountered within the pre-alpidic Serbo-Macedonian Massif as intermediate and acid fissure eruptions following the regional NW—SE tectonic lineaments. Rhyolites with high potassium contents with K/Na ratios of 5 to 30 and lower than 1–2 wt % Na_2O occur in some parts of the world. They are marked by large amounts of SiO_2 , low CaO content and, in many cases low Al_2O_3 [37]. Rhyolites from the Okinawa Trough (China), are derived from a cryptic potassium-rich source [6]. The South Aegean Volcanic Arc is an area of the complex convergent and collisional system of the Eurasia and Africa plates. It has been shown that granitic and rhyolitic melts can be generated entirely from crustal melts without the contribution of mantle components, namely by biotite dehydration melts of immature sediments at lower crustal pressure [34]. Examples of late Miocene crust-derived granites and rhyolites both exist in the southern Aegean, on the other hand, examples of high-K basaltic andesites and shoshonites in western Anatolia have shown to have been generated by melts in the mantle [12]. During recent fieldwork in the Herson—Kilkis area, volcanic

Fig. 1 Location map showing the main structural features of northern Greece and sampling sites



rocks were found in the volcano-sedimentary series around Kilkis area. This study presents new geochemical data and further contributes to the discussion of the petrogenesis of this group of volcanic rocks.

2 Geological setting

The Rhodope massif comprises a Variscan high-grade metamorphic basement and a low-grade metamorphic cover, which encompasses a subduction-accretion complex from the late Jurassic to the early Cretaceous period (Fig. 1) [11]. The rocks are covered by a sedimentary layer that was formed during the late Cretaceous to early Neogene period in a way that is not in alignment with the underlying rocks. The Rhodope massif was once part of the Eurasian continent but later became detached due to the formation of a back-arc basin during the early Mesozoic era. This basin formed on the upper plate of the subduction zone located on the northern side of the Tethys Ocean. The ocean basin was closed as a result of the Eo-Alpine contractional event that occurred in the early Cretaceous period. The Axios zone comprises Paleogene oceanic material, such as ophiolites, that is associated with the former Vardar Ocean [11] (Fig. 1). The Serbo-Macedonian massif is a Variscan metamorphic massif that shares similarities with the basement of the Rhodope Massif [11]. The Serbo-Macedonian massif has been divided into two series [21, 22] (Fig. 1): (a) a terrane which is composed largely of migmatitic gneisses, but with minor amphibolites and two major marble units, and (b) a terrane which is composed of schists, gneisses and amphibolites.

According to previous studies [5, 10, 24, 31], the volcanic unit is part of the autochthonous Svoula series, which lies between the Serbo-Macedonian Massif and the Axios zone to the west (Fig. 1). The geological sequence within the Svoula series is the following (from bottom to top) [24]: (a) Volcano-sedimentary Lower Triassic series, (b) Limestones Middle and Upper Triassic; and (c) Limestones Lower and Middle Jurassic. The Svoula series includes the following rock types: sedimentary rocks subjected to low-grade regional metamorphism, volcano-sedimentary rocks, ophiolites and greenschists. Tectonic contact exists between the volcano-sedimentary rocks and the Palaeozoic Vertiskos two-mica gneisses of the Serbo-Macedonian massif to the east.

The western contact with limestones is also tectonic. More details about the geology and tectonic setting of the volcano-sedimentary series are given by Kockel and Walther [23], Chatzidimitriadis [5] and Kelepertsis et al [18].

3 Materials and Methods

Sixteen samples were collected from various occurrences of the volcanic rocks around Kilkis town (Fig. 1). All of the rock samples were examined in thin sections, and further mineralogical information for some of them was obtained by X-ray diffraction. The rock samples were analyzed for major and trace elements by XRF. FeO was determined by a chemical method and loss on ignition (LOI) was determined by heating to 1000 °C. The analytical results are presented in Table 1, and the maximum relative errors are 1% for SiO₂, 5% for Al₂O₃ and K₂O and 10% for all other constituents, except trace elements below about 20 mg Kg⁻¹ (relative error about 20%). The CIPW norm calculations were presented in Table 2.

4 Results

4.1 Petrography-Mineralogy

The acid volcanic rocks of the Pyrgoto—Kilkis area consist of massive to foliated rocks of various colors, including pink, grey and grey-green [17]. Four rock samples (X22, X23, X3 and X16) are rhyolitic tuffs consisting of an aphanitic groundmass of quartz and feldspars. One rock sample (X21) may be an ignimbrite, consisting of a dark aphanitic matrix with very fine-grained sericite, quartz, feldspar and opaque minerals. The matrix has a primary flow texture. The Herson-Kilkis lavas are typically porphyritic, with phenocrysts of alkali feldspar and quartz in a groundmass of feldspar, frequently altered to sericite. Magnetite and pyrite occur as opaque idiomorphic crystals, most of which have been altered to hematite. From Fig. 2, where the normative feldspar compositions are shown, it is evident that the feldspars in most of the samples are close to orthoclase compositions, with only three samples showing a significant albite component. The O-Ab-Or plot also shows that most of the rhyolitic rocks studied are composed of orthoclase and quartz, confirmed by X-ray diffraction (Fig. 2). A complete list of Herson rock samples is included in Appendix A.

Table 1 Major element (wt %) and trace element (mg Kg⁻¹) contents of the Herson rocks (ND: Not Detected)

	X1	X4	X8	X9	X13	X16	X18	X19	X21	X22
SiO ₂	75.23	75.73	74.18	82.61	69.51	75.64	80.27	75.69	71.36	75.62
Al ₂ O ₃	13.68	12.16	13.69	0.68	16.21	12.54	9.52	12.26	14.09	12.48
Fe ₂ O ₃	0.24	0.38	0.90	12.79	0.76	0.84	0.55	0.70	1.08	0.65
FeO	0.27	0.43	1.01	2.00	0.87	0.83	0.63	0.79	1.21	0.73
MgO	0.36	0.21	0.65	0.24	0.61	0.33	0.22	0.72	0.23	0.23
CaO	0.07	0.06	0.16	0.05	0.07	0.05	0.05	0.09	0.05	0.04
Na ₂ O	3.10	0.51	3.95	0.31	1.99	1.45	0.40	1.67	0.49	1.41
K ₂ O	6.89	9.45	3.97	0.16	8.42	7.33	7.21	7.02	10.66	8.08
TiO ₂	0.24	0.54	0.47	0.03	0.26	0.19	0.21	0.19	0.31	0.26
P ₂ O ₅	0.02	0.08	0.11	0.23	0.03	0.05	0.04	0.05	0.03	0.03
LOI	0.38	0.55	0.94	1.33	1.32	0.80	0.98	0.86	0.46	0.48
Total	100.48	100.10	100.03	100.43	100.05	100.05	100.08	100.04	99.97	100.01
Nb	41	26	19	ND	22	25	32	27	41	22
Zr	404	281	332	30	230	185	192	157	222	208
Y	87	63	53	10	67	61	58	66	78	68
Sr	17	28	20	ND	8	27	134	6	18	8
Rb	115	242	139	ND	263	221	145	247	240	237
Zn	38	58	52	81	74	31	43	94	51	57
Cu	ND	ND	ND	338	ND	ND	21	6	ND	ND
Ni	ND	6	6	ND	5	13	8	9	6	8
Cr	21	24	24	19	22	21	15	21	19	20
Ce	107	78	45	16	86	III	71	116	119	102
Nd	87	43	24	5	46	51	48	65	70	53
La	61	33	18	9	43	55	21	67	52	46
Ba	406	1445	470	332	713	669	10,859	132	2472	554
Sc	ND	8	6	ND	9	11	7	9	12	7
	X23	X24	X26	X34	X38	X39	Average	A	B	C
SiO ₂	76.85	73.60	73.31	70.40	72.67	71.73	74.12	72–75.77	71.48	75.29
Al ₂ O ₃	12.19	13.87	13.37	14.32	14.39	13.69	13.23	12–13.69	15.32	12.97
Fe ₂ O ₃	0.34	0.65	0.76	1.19	0.61	1.01	0.71	0.34–1.40	0.63	0.97
FeO	0.38	0.73	0.87	1.35	0.70	1.15	0.80	0.01–0.96	0.32	0.14
MgO	0.21	0.20	0.56	0.67	0.16	0.73	0.39	0.11–0.74	0.48	0.05
CaO	0.06	0.05	0.12	0.14	0.08	0.14	0.08	0.69–2.36	0.35	0.04
Na ₂ O	1.21	2.14	0.81	0.94	1.88	0.42	1.49	314.18	151	0.55
K ₂ O	7.93	8.40	8.56	9.47	8.88	9.74	8.13	3–4.60	8.42	9.00
TiO ₂	0.26	0.26	0.24	0.34	0.21	0.36	0.30	0.09–0.26	0.29	0.04
P ₂ O ₅	0.03	0.08	0.08	0.08	0.06	0.09	0.07	0.01–0.09	0.05	0.02
LOI	0.60	0.21	1.37	1.05	0.36	0.90	0.75	0.40–4.93	1.17	0.88
Total	100.11	100.19	100.05	99.95	100.00	99.96	100.07	100.02	99.95	100.19
Nb	24	21	28	17	21	20	26			
Zr	68	191	118	237	120	254	222	86		
Y	19	48	52	56	40	61	62	25		
Sr	245	28	83	ND	ND	11	21			
Rb	245	256	332	328	317	358	246	102		
Zn	215	27	18	124	24	101	68			
Cu	ND	ND	ND	ND	ND	10				
Ni	11	6	9	ND	13	8	7			
Cr	22	24	20	21	24	23	21			
Ce	92	78	58	66	54	77	84	46		

Table 1 (Continued)

	X23	X24	X26	X34	X38	X39	Average	A	B	C
Nd	49	41	38	32	28	41	48	16		
La	49	46	22	24	24	39	40	25		
Ba	452	592	6728	126	126	513	1049			
Sc	7	7	5	6	6	6	7			

A: Range for rhyolites from Milos island; B: Average for rhyolites from Alexandroupolis area; C: Average for alkali rhyolites from Kilkis area

4.2 Geochemistry

The analytical results are reported in Table 1 and plotted on several variation diagrams (Figs. 3, 4, 5, 6, 7, 8, 9, 10, 11, 12, 13). In the TAS classification diagram, the Herson rock samples fall within the field of Rhyolite (Fig. 3); while in the SiO_2 vs Nb/Y diagram, most of the Herson rock samples fall within the Rhyolite field (Fig. 4). The least altered Herson rocks plot toward the centre of the diagram; while hydrothermally altered Herson rocks plot at positions near to K-feldspar which is the principal hydrothermal mineral present (Fig. 5). The weathering of Herson presents a compositional linear trend extending from the W vertex to F vertex (Fig. 6a). Increasing F values of Herson rock samples represent the abundance of felsic materials (Fig. 6b). The Q-Ab-Or diagram shows the plots of Herson rock samples concerning quartz-feldspar cotectics (Fig. 7). As sample number X9 has been altered by mineralizing fluids, it is excluded from the geochemical diagrams and the following discussion. Using the K_2O — SiO_2 diagram of Peccerillo and Taylor [35], the rocks are all classified as high-k rhyolites (Fig. 8). The samples show a wide range of K_2O contents with one below 4% and the others in the range 6.89–10.66% K_2O . Although the K_2O contents are exceptionally high for rhyolites, the samples are either sub-alkaline or only slightly alkaline on the $(\text{Na}_2\text{O} + \text{K}_2\text{O})$ versus Si_2O diagram (Fig. 9); this is because only three samples have Na_2O contents greater than 2% (Table 1). Apart from sample X8, the $\text{K}_2\text{O}/\text{Na}_2\text{O}$ ratios are all higher than one; the range is 2.2–22 and the average is 5.5. In the AFM diagram (Fig. 10) most of the samples lie below the field of typical calc-alkaline rocks due to their relatively low total iron / MgO ratios.

The differentiation index (O + Or + Ab) is high (range 92–97) (Table 2), and typical of rhyolitic rocks. The values of several major elements, especially the high K_2O and the low CaO and Na_2O contents, distinguish the Herson—Kilkis rhyolites from those of the calc-alkaline series from active continental margins [7]. Similar differences also occur concerning the rhyolitic rocks from the South Aegean active arc [8, 14, 15, 33], Kelepertsis and Reeves [19] and Afyon, Central Anatolia [20]. On the other hand, there is a close similarity between the Herson Kilakis rhyolites and rhyolites from the Alexandroupolis area, eastern Greece [1, 8] as far as K_2O and Na_2O are concerned (Table 1).

Most rock samples are distinctly peraluminous, with normative corundum (Table 2) greater than 1% in all rhyolite samples except X4 and greater than 1.5% for 60% of the rhyolites. In addition, the molecular ratio $\text{Al}_2\text{O}_3/(\text{CaO} + \text{Na}_2\text{O} + \text{K}_2\text{O})$ exceeds 1.0% in all cases and is greater than 1.1% for 80% of the rock samples. The low values of Sr, Ni and Cr (Table 1) reflect the absence of plagioclase and mafic minerals and Cu is very low in all samples except one (X9) affected by mineralization. Apart from three samples (X4, X21 and X8, the latter not plotted), Fig. 11 shows the strong correlation between K_2O and Rb in the Herson—Kilkis rocks. TiO_2 , and Zr also show a good correlation (Fig. 12). The Ba contents are very variable, suggesting that Ba-rich fluids may have affected some of the rocks. Nb, Ce, La, Nd and Y (Table 1) are significantly higher than in rhyolites from the South Aegean volcanic arc [14]. Apart from one sample (X18) the Herson rhyolites have high Rb/Sr ratios, with values ranging from 4 to greater than 30. The unusual composition of Herson rocks is further emphasised by their extremely low CaO contents, ranging from 0.04 to 0.16% (Table 1 and Fig. 13).

5 Discussion

5.1 Genesis of volcanic rocks of the study area

Kelepertsis et al. [18] assigned the ultrapotassic rocks from the nearby Pyrgoto area (Fig. 1) to a shoshonitic series. The Pyrgoto rocks are less siliceous, generally 63–70% SiO_2 , than those reported here and are classified as K-rich trachytes (most samples having K_2O contents of 7–12%) by the K_2O — SiO_2 diagram of Peccerillo and Taylor [35]. Rocks with shoshonitic

Table 2 CIPW norms of the Herson-Kilkis rocks (*Thornton – Tuttle index [39])

	X1	X4	X8	X9	X13	X16	X18	X19	X21	X22	X23	X24	X26	X34	X38	X39
Q	30.15	35.97	35.06	80.74	24.74	38.67	50.31	37.96	27.09	36.16	38.92	28.47	35.14	27.41	27.31	30.82
Co	1.03	0.95	2.88	0.01	3.80	2.23	1.07	1.87	1.73	1.42	1.49	1.23	2.78	2.48	1.68	2.44
Or	40.67	56.16	23.72	0.95	50.45	43.71	43.05	41.87	63.37	47.96	47.18	49.62	51.34	56.69	52.75	58.16
Ab	26.24	4.99	33.80	2.63	17.11	12.37	3.39	14.31	4.15	12.02	10.75	18.12	6.94	8.05	16.00	3.56
An	0.22	0.00	0.07	0.00	0.15	0.00	0.00	0.12	0.05	0.01	0.10	0.07	0.07	0.17	0.01	0.11
Hy	0.90	0.52	1.96	0.60	2.08	1.34	0.90	2.37	1.39	0.95	0.52	0.87	1.99	2.63	0.83	2.52
Il	0.46	0.91	0.91	0.06	0.49	0.36	0.40	0.36	0.59	0.49	0.49	0.49	0.46	0.65	0.40	0.68
Hm	0.10	0.38	0.00	8.40	0.00	0.00	0.00	0.00	0.00	0.00	0.01	0.00	0.00	0.00	0.00	0.00
Ap	0.05	0.11	0.25	0.09	0.07	0.09	0.09	0.12	0.07	0.07	0.07	0.19	0.19	0.19	0.14	0.21
DI*	97.05	97.13	92.59	84.31	92.30	94.75	96.75	94.14	94.62	96.15	96.85	96.21	93.42	92.16	96.07	92.54

Fig. 2 Normative feldspar composition (Or-Ab-An) of Herson rock samples (•)

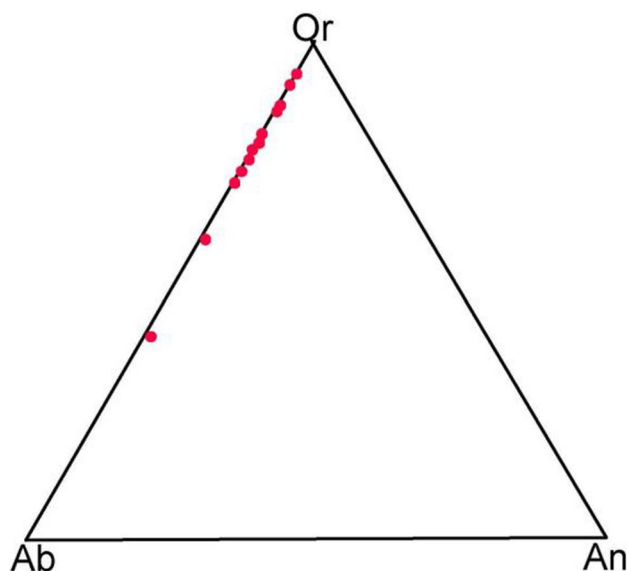
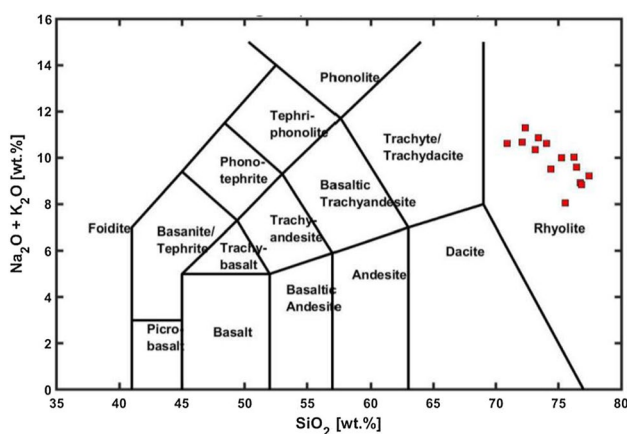


Fig. 3 TAS classification diagram for Herson rock samples. The boundaries and nomenclature are from Le Bas et al. [28]



affinities are commonly associated with Oligocene to Quaternary calc-alkaline volcanism in and around the Aegean Sea area and Western Anatolia [9].

These shoshonitic rocks, in which K₂O rarely exceeds 6% and intermediate rock-types predominate, are believed to have originated from mantle sources mainly in or near subduction zones but some occurrences are associated with tensional tectonic settings within plates or at non—convergent plate margins [9, 26]. The compositional spectrum of the

Fig. 4 SiO₂ vs Nb/Y classification diagram for Herson rock samples. The boundaries and nomenclature are from Winchester and Floyd [41]

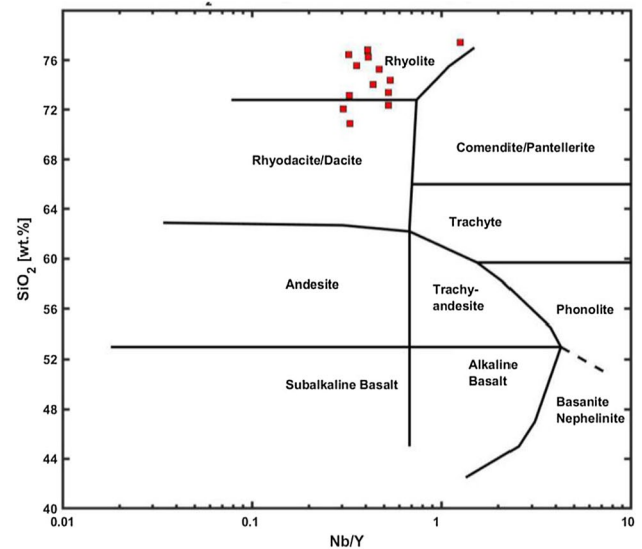
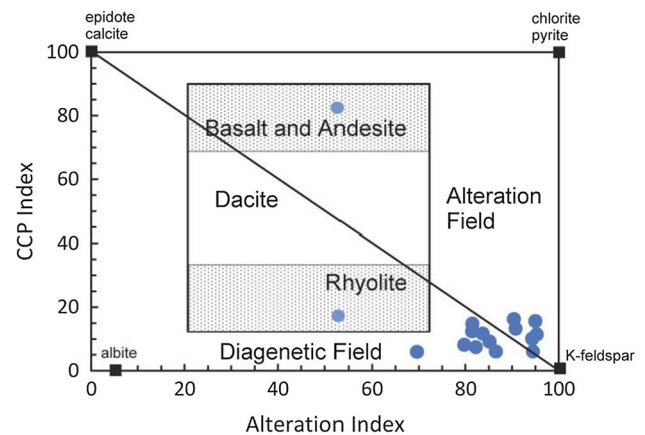


Fig. 5 The alteration box-plot for the Herson rock samples. The boundaries and nomenclature are from Large et al. [27]



Aegean region shoshonitic occurrences includes high—K varieties of the basaltic andesite-dacite range in addition to shoshonite, latite, trachyte and high-K rhyolite. In sharp contrast, however, the volcano-sedimentary series in northern Greece (Fig. 1) is thought to be of Triassic age and consists almost entirely of trachytes and rhyolites with very high K₂O contents, 6–12% [18], although there are a few examples of normal dacite and rhyolite. This restricted compositional range and K₂O contents, which are uniquely high for the entire Aegean region show that the magmas of the Kilikis area were produced by processes significantly different from those which give rise to most examples of shoshonitic association.

It is clear from the previous section that the geochemistry of the source material for the Herson Kilikis rhyolites had an extreme composition. Several of the geochemical characteristics of these rocks show that their parentage has a significant component derived from a sedimentary source. The most striking evidence of the S-type properties [4] of these rhyolites are: (a) the K₂O/Na₂O ratios (2.2–22) are extremely high and greater than 5 in 60% of the samples; (b) normative corundum exceeds 1.5% in 60% of the samples; (c) in 80% of the samples studied the molecular ratio Al₂O₃ / (CaO + Na₂O + K₂O) exceeds 1.1; (d) the Rb/Sr values range from 4 to 40, exceeding 5 in 85% and 10 in 50% of the samples; and (e) the CaO (0.04–0.16%) and Sr (range 0–83 mg Kg⁻¹, average 19 mg Kg⁻¹, excluding sample X18) contents are very low.

Rhyolites from the Antiparos island (Cyclades) and Izmir (W. Anatolia) have initial Sr—isotope ratios of 0.711–0.712 [3, 13], which are indicative of a crustal melting origin. These rhyolites and similar ones from Afyon (W. Anatolia) [20], have an undoubted crustal origin but their geochemical characteristics are fully compatible with an igneous source, i.e. they have I-type properties. Isotopic data are not available for the Herson—Kilikis rhyolites but these are considerably more extreme in their geochemistry, particularly their higher K₂O/Na₂O ratios, lower Ca contents and distinctly peraluminous nature, and the general geochemical evidence indicates that they were produced by anatexis of source rocks with a large sedimentary component. It should also be noted that in addition to K₂O, the Herson—Kilikis rhyolites are considerably

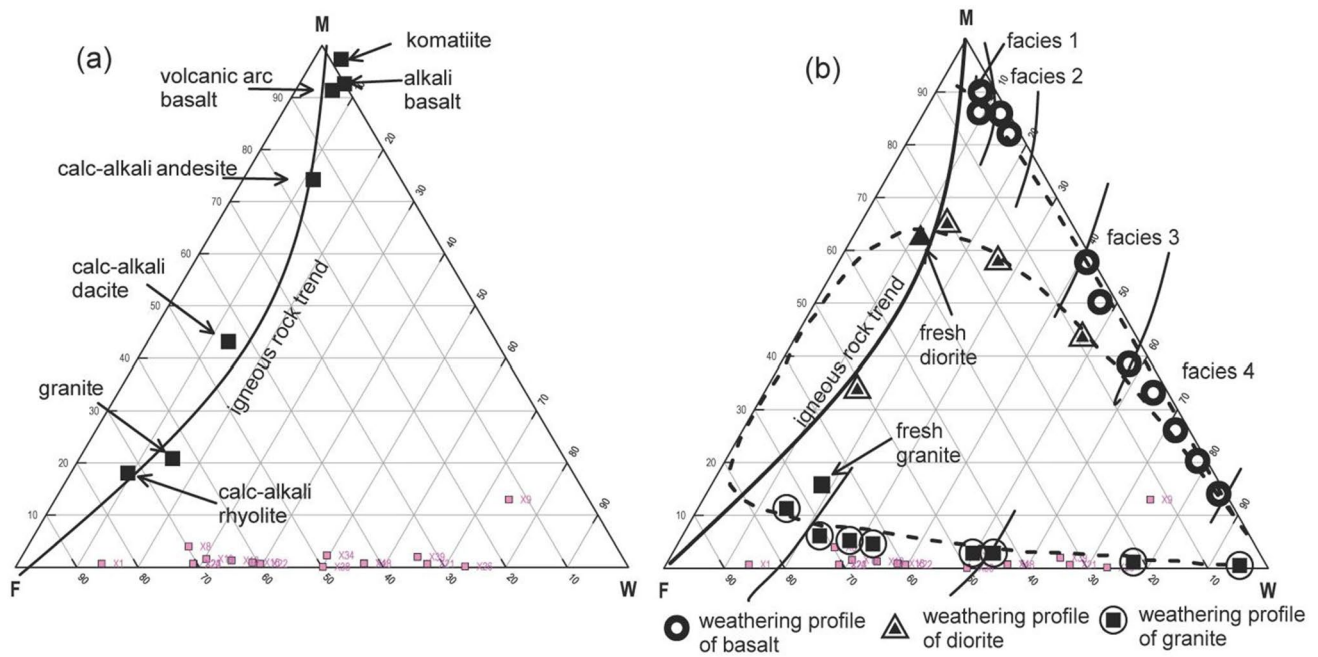
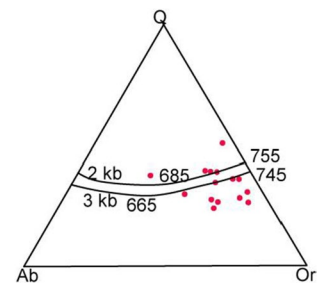


Fig. 6 MFW ternary plot for Herson rocks (a); and weathering profiles (b). The boundaries and nomenclature are from Ohta and Arai [32] (red square: Herson rock sample)

Fig. 7 Plot of Q-Ab-Or for volcanic rocks of Herson (•). Temperatures in °C, quartz cotectic (2 kb), feldspar cotectic (3 kb), experimental data from Tuttle and Bowen [40]



more enriched, by a factor of about 2, in the elements Rb, Y, La, Ce, Nd and Zr than rhyolites, e.g. Milos (Table 1), produced by fractionation of a mantle-derived partial melt.

Biotite-bearing gneisses and schists are the predominant rock—types in the Serbo—Macedonian Massif (Fig. 1). The gneisses and schists are rather variable, but the presence of significant amounts of argillaceous material is indicated by the high proportion of rocks, including two-mica varieties, of pelitic origin. In the presence of quartz, which is common in the schists and gneisses of the basement, muscovite, biotite, and quartz may take part in several reactions, which are dependent on pressure (P), temperature (T) and the H₂O content of the system. When H₂O is present, the most likely situation, muscovite and quartz react when T exceeds 580 °C at 1 kb and 660 °C at 3 kb and melting begins at 730 °C for 1 kb and 670 °C for 3 kb [42]. At pressures greater than 3.5 kb melting begins at 670 °C and as P increases, the temperature at which melting begins decreases by about 20 °C per kb. The presence of biotite has only a small effect on the P and T of reaction but cordierite or garnet would be added to the reaction products. Without muscovite, the quartz-biotite reaction occurs at significantly higher temperatures.

At temperatures ranging from 650 to 700 °C and pressures varying between 3 and 6 kb in the presence of water the composition of the partial melts would lie some distance away from the minimum melting composition in the Q—Or—Ab system [29, 40]. Thus, under these conditions schists and gneisses containing abundant quartz and muscovite, would undergo substantial amounts of partial melting. Such melts would be enriched in the components of K-feldspar, quartz and, if present in the source rocks, Ab-rich plagioclase [42]. In a plagioclase—poor quartz—muscovite—schist the bulk composition would lie towards the Q—Or side of the system (Fig. 7) and substantial partial melts would be rich in quartz and K-feldspar components. Eight of the Herson rock samples in Fig. 7 are plotted close to quartz-feldspar cotectics for

Fig. 8 K_2O - SiO_2 relationship for the Herson volcanic rocks (•). The boundaries and nomenclature are from Peccerillo and Taylor [35]

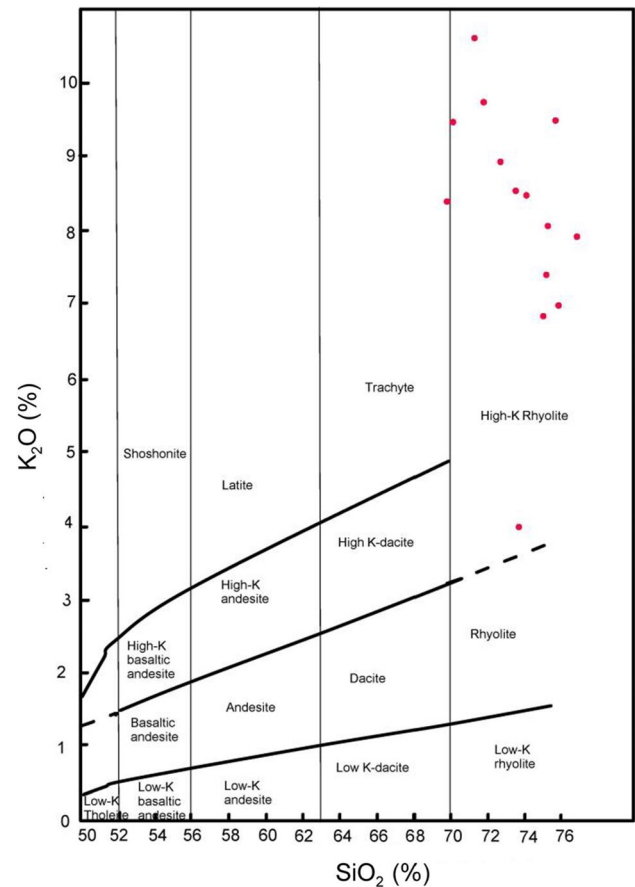
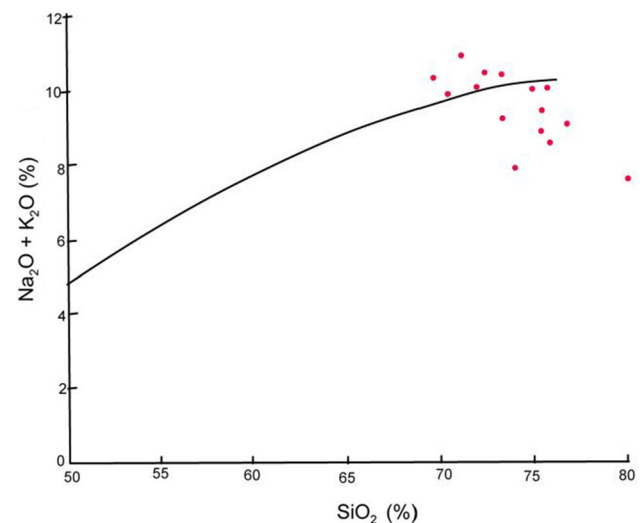


Fig. 9 Alkali vs. silica plot for Herson-Kilkis volcanic rocks (•). Dividing line between alkaline and sub-alkaline fields after Irvine and Baragar [16]



2 and 3 kb, one sample is plotted in the quartz field, while the others fall within the K-feldspar field and would continue to do so even at 10 kb. Samples lying close to the medium-pressure cotectics probably formed directly by partially melting basement rocks, while accumulation of K-feldspar is likely to have occurred in those in the K-feldspar field. Other factors contributing to the compositional range could be the following: source rock heterogeneity, variable degrees of partial melting and the effects of other phases. The generation of the Herson—Kilkis magmas may be attributed to the Triassic—Jurassic orogenic events, which produced deformation and the intrusion of a series of granitic plutons along an NW-SE trending zone running from Sithonia to Yugoslavia.

Fig. 10 AFM plot for the analysed rock samples (*). The lines delineate the area of typical calc – alkaline rocks

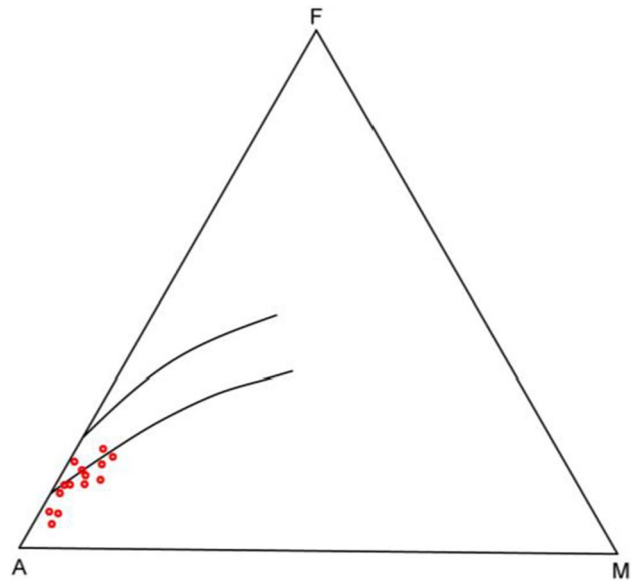


Fig. 11 K₂O vs Rb diagram for volcanic rocks (*) from the Herson area

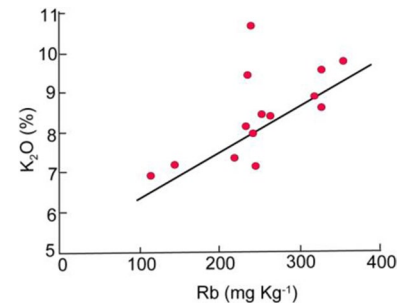


Fig. 12 TiO₂ vs Zr plot for volcanic rocks (*) from the Herson area

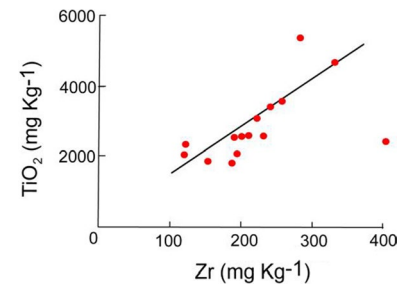
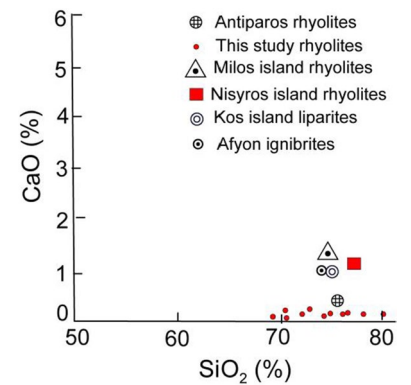


Fig. 13 CaO vs SiO₂ diagram for volcanic rocks (*) from the Herson area



6 Conclusions

Herson-Kilkis lavas are porphyritic with alkali feldspar and quartz phenocrysts in feldspar, often changed to sericite, and quartz. Most opaque idiomorphic magnetite and pyrite crystals are hematite. Most samples have orthoclase feldspar compositions, with only three having a considerable albite component. The O-Ab-Or plot and X-ray diffraction demonstrate that most rhyolitic rocks are formed from orthoclase and quartz. The Herson rocks that have been affected by hydrothermal processes are found closer to the K-feldspar, which is the main mineral associated with hydrothermal alteration. The weathering of Herson exhibits a linear trend in composition. The rocks' chemistry involves high K_2O (7–12%), K_2O/Na_2O (2–22), low CaO (0.04–0.16%), Sr (0–83 mg Kg^{-1}), and Rb/Sr (4–40). Rhyolites formed from a more basic magma by low-pressure fractional crystallization have lower trace elements Nb, Nd, Ce, La, Rb, and Y. Most rock samples are clearly peraluminous, with normative corundum concentration greater than 1% in all rhyolite samples. The Herson-Kilkis rhyolites were crystallized by an acid magma formed by the partial fusing of K-rich schists or para-gneisses along a dip-slip fault at the western edge of the Serbo-Macedonian massif.

Author contributions A.E.K.; methodology, D.E.A.; software, A.E.K.; validation, A.E.K. and D.E.A.; formal analysis, D.E.A. and A.E.K.; investigation, A.E.K.; resources, A.E.K., D.E.A.; data curation, A.E.K.; writing—original draft preparation, A.E.K., D.E.A.; writing—review and editing, A.D.A.; visualization, A.E.K.; supervision, A.E.K.; project administration, A.E.K. All authors have read and agreed to the published version of the manuscript.

Funding This research received no external funding.

Data availability The data used in this study is available upon reasonable request by contacting the authors at the following email address: kelepertsis@geol.uoa.gr.

Declarations

Ethics approval and consent to participate Not applicable.

Consent to participate Not applicable.

Competing interests The authors declare no conflict of interest.

Open Access This article is licensed under a Creative Commons Attribution 4.0 International License, which permits use, sharing, adaptation, distribution and reproduction in any medium or format, as long as you give appropriate credit to the original author(s) and the source, provide a link to the Creative Commons licence, and indicate if changes were made. The images or other third party material in this article are included in the article's Creative Commons licence, unless indicated otherwise in a credit line to the material. If material is not included in the article's Creative Commons licence and your intended use is not permitted by statutory regulation or exceeds the permitted use, you will need to obtain permission directly from the copyright holder. To view a copy of this licence, visit <http://creativecommons.org/licenses/by/4.0/>.

Appendix A

Petrographic description and locations of the rock samples of the study area.

X1: Quartz—porphyry rock with a fluidal texture. Phenocrysts of K—feldspar (sanidine) and quartz with a microcrystalline groundmass consisting of quartz and feldspars

X4: Rhyolitic rock, intensively altered

X8: Quartz—porphyry rock with a fluidal texture. X9. Quartz—rich rock, altered by mineralizing fluids

X13: Quartz—porphyry rock like X1. Phenocrysts of K—feldspar altered to sericite

X16: Rhyolitic tuff with a fluidal texture

X18: Quartz—porphyry rock consisting of phenocrysts of K—feldspar and quartz and small grains of quartz, feldspars and sericite. Trace amounts of hematite and magnetite occur as opaque minerals.

X21: Rhyolitic ignimbrite with a dark groundmass of very small grains of sericite, quartz, feldspar and opaque minerals. The rock shows a primary fluidal texture

X22: Rhyolitic tuff; none of the minerals can be determined under the microscope

X23: Rhyolitic tuff similar to X22

X24: Typical quartz—porphyry, like X1 and X13

X26: Quartz—porphyry. Fine—grained groundmass and phenocrysts of quartz and K—feldspars. Quartz crystals are in the form of hexagonal sections

X34: Quartz – porphyry

X38: Quartz—porphyry

X39: Quartz—porphyry

References

1. Arikas K. Geologische und petrographische Untersuchungen in der Umgebung von Kirki (Thrazien, Griechenland), Mitt. Geo-/Palaont. inst. Univ. Hamburg 4;1979.
2. Ayalew D, Ishiwatari A. Comparison of rhyolites from continental rift, continental arc and oceanic island arc: implication for the mechanism of silicic magma generation. *Island Arc*. 2011;20(1):78–93. <https://doi.org/10.1111/j.1440-1738.2010.00746.x>.
3. Borsi S, Ferrara G, Innocenti F, Mazzuoli R. Geochronology and petrology of recent volcanics in the eastern Aegean Sea (West Anatolia and Lesvos Island). *Bull Volcanol*. 1972;36:473–96. <https://doi.org/10.1007/BF02597122>.
4. Chappell BW, White AJR. Two contrasting granite types. *Pacific Geo*. 1974;8:173–4.
5. Chatzidimitriadis E. Die geologische Untersuchung der Gebiete Valti Bei Kilikis und Aswestochori bei Thessaloniki, ein petrolo-gishtechnischer Vergleich. *Praktika of Academy of Athens*. 1980;54:458–88.
6. Chen Z, Zeng Z, Yin X. Petrogenesis of highly fractionated rhyolites in the southwestern Okinawa Trough: Constraints from whole-rock geochemistry data and Sr–Nd–Pb–O isotopes. *Geol J*. 2019;54:316–32. <https://doi.org/10.1002/gj.3179>.
7. Ewart A. A review of the mineralogy and chemistry of Tertiary–Recent dacitic, latitic, rhyolitic, and related salic volcanic rocks. In: *Developments in Petrology*, 1979; 6:13–121. <https://doi.org/10.1016/B978-0-444-41765-7.50007-1>.
8. Fytikas M, Innocenti F, Kolios N, Manetti P, Mazzuoli B, Poli G, Rita F, Villari L. Volcanology and petrology of volcanic products from the island of Milos and neighbouring islets. *J Volcanol Geotherm Res*. 1986;28:297–317. [https://doi.org/10.1016/0377-0273\(86\)90028-4](https://doi.org/10.1016/0377-0273(86)90028-4).
9. Fytikas M, Innocenti F, Manetti P, Mazzuoli P, Peccerillo A, Villari L. Tertiary to Quaternary evolution of volcanism in the Aegean region. *Geol Soc Lond Spec Publ*. 1984;17:687–99. <https://doi.org/10.1144/GSL.SP.1984.017.01.55>.
10. Fytikas M, Mazzuoli R, Peccerillo A, Villari L. Neogene volcanism of the Northern and Central Aegean Region. *Ann Geol des Pays Hell*. 1979;30:106–29.
11. Park G. *The Making of Europe. A Geological History*. 1st ed., Liverpool University Press; 2014.
12. Innocenti F, Agostini S, Di Vincenzo G. Neogene and Quaternary volcanism in Western Anatolia: Magma sources and geodynamic evolution. *Mar Geol*. 2005;221:397–421. <https://doi.org/10.1016/j.margeo.2005.03.016>.
13. Innocenti F, Kolios N, Manetti P. Acid and basic late neogene volcanism in central aegean sea: Its nature and geotectonic significance. *Bull Volcanol*. 1982;45:87–97. <https://doi.org/10.1007/BF02600426>.
14. Innocenti F, Manetti P, Peccerillo A, Poli G. South Aegean volcanic arc: Geochemical variations and geotectonic implications. *Bull Volcanol*. 1981;44:377–91. <https://doi.org/10.1007/BF02600571>.
15. Innocenti F, Manetti P, Peccerillo A, Poli G. Inner arc volcanism in NW Aegean arc: geochemical and geochronological data. *N Jh Miner Mh*. 1979;4:145–58.
16. Irvine TN, Baragar WRA. A Guide to the chemical classification of the common volcanic rocks. *Can J Earth Sci*. 1971;8:523–48. <https://doi.org/10.1139/e71-055>.
17. Kelepertsis AE, Andrulakis J. Litho-geochemical studies of barite mineralization in the Kilikis area, northern Greece. *Praktika of the Athens Academy*. 1981;63:272–87.
18. Kelepertsis A, Chatsidimitriadis E, Andrulakis J. Geology, geochemistry and tectonic setting of the volcano-sedimentary series, Kilikis - Central Macedonia, Greece. *Chem der Erde*. 1985;44:151–74.
19. Kelepertsis A, Reeves R. The Geochemistry of the Volcanic Rocks of Kos Island, Aegean Sea, Greece. *Ann Geol Pays Hellen*. 1987;33:443–62.
20. Keller J, Villari L. Rhyolitic ignimbrites in the region of Afyon (Central Anatolia). *Bull Volcanol*. 1972;36:342–58. <https://doi.org/10.1007/BF02596876>.
21. Kockel F, Mollat H, Walther HW. Geologie des Serbo-Mazedonischen Massivs und seines mesozoischen Rahmens (Nord Griechenland): *Geol. Jb*. 1971;89:529–51.
22. Kockel F, Mollat H, Walther HW. Erläuterungen zur geologischen Karte der Chalkidiki und angrenzender Gebiete 1:100.000 (Nord-Griechenland): Bundesanstalt für Geowissenschaften und Rohstoffe, Hannover; 1977. pp119.
23. Kockel F, Walther H (1977) Erläuterungen zur Geologischen Karte der Chalkidiki und angrenzender Gebiete 1:100.000 (Nord - Griechenland).
24. Kockel F, Ioannidis K. Geological Map of Greece. Kilikis sheet (1:50.000), Institute of Geology and Mineral Exploration (IGME), Athens;1979.
25. Kockel F, Mollat H, Gundlach H. Hydrothermally altered and (copper) mineralized porphyritic intrusions in the Serbo-Macedonian Massif (Greece). *Miner Deposita*. 1975;10:195–204. <https://doi.org/10.1007/BF00207136>.
26. Kolios N, Innocenti F, Manetti P, Peccerillo A, Giuliani O. The pliocene volcanism of the voras Mts (Central Macedonia, Greece). *Bull Volcanol*. 1980;43:553–68. <https://doi.org/10.1007/BF02597692>.
27. Large R, Gemmill B, Paulick H. The alteration box plot: a simple approach to understanding the relationship between alteration mineralogy and litho-geochemistry associated with volcanic-hosted massive sulfide deposits. *Economic Geology*. 2001;96:957–71.
28. Le Bas MJ, Le Maitre RW, Streckeisen A, Zanettin B. A chemical classification of volcanic rocks based on the total alkali-silica diagram. *J Petrol*. 1986;27(3):745–50.
29. Luth WC, Jahns RH, Tuttle OF. The granite system at pressures of 4 to 10 kilobars. *J Geophys Res*. 1964;69:759–73. <https://doi.org/10.1029/JZ069i004p00759>.
30. Melidonis NG. Der Bogen junger vulkanischer Gesteine zwischen Strymonikon und Metamorphosis (Mazedonien). *Mineral Exploration* 5, I.G.S.R., Athens,1972. p 51. (in Greek).

31. Mercier J. Paleogeographie, orogenese, metamorphisme et magmatisme des zones internes des Hellenides en Macedonie (Grece): Vue d'ensemble. *Bull Geol Soc France*. 1966;8:1020–49.
32. Ohta T, Arai H. Statistical empirical index of chemical weathering in igneous rocks: A new tool for evaluating the degree of weathering. *Chem Geol*. 2007;240:280–97.
33. Paola GM. Volcanology and petrology of Nisyros Island (Dodecanese, Greece). *Bull Volcanol*. 1974;38:944–87. <https://doi.org/10.1007/BF02597100>.
34. Patino Douce AE, Beard JS. Effects of P, f (O₂) and Mg/Fe ratio on dehydration melting of model metagreywackes. *J Petrol*. 1996;37:999–1024. <https://doi.org/10.1093/petrology/37.5.999>.
35. Peccerillo A, Taylor SR. Geochemistry of eocene calc-alkaline volcanic rocks from the Kastamonu area, Northern Turkey. *Contrib Mineral Petrol*. 1976;58:63–81. <https://doi.org/10.1007/BF00384745>.
36. Philpotts A, Ague J. *Principles of Igneous and Metamorphic Petrology*. Cambridge: Cambridge University Press; 2009.
37. Popov VS, Nikolayenko YuS. The Origin of Ultrapotassic Rhyolites. *IntGeolRev*. 2010;30:540–50. <https://doi.org/10.1080/00206818809466034>.
38. Streck MJ, Swenton VM, McIntosh W, Ferns ML, Heizler M. Columbia River rhyolites: age-distribution patterns and their implications for arrival, location, and dispersion of continental flood basalt magmas in the crust. *Geosciences*. 2023;13:46. <https://doi.org/10.3390/geosciences13020046>.
39. Thornton CP, Tuttle OF. Chemistry of igneous rocks—[Part] 1, Differentiation index. *Am J Sci*. 1960;258:664–84. <https://doi.org/10.2475/ajs.258.9.664>.
40. Tuttle OF, Bowen NL. Origin of granite in the light of experimental studies in the system NaAlSi₃O₈ - KAlSi₃O₈ - SiO₂ - H₂O. *Geol Soc Am Mem*. 1958;74:1–146.
41. Winchester JA, Floyd PA. Geochemical discrimination of different magma series and their differentiation products using immobile elements. *Chem Geol*. 1977;20:325–43.
42. Winkler HGF. *Petrogenesis of Metamorphic Rocks*. New York: Springer - Verlag; 1979.

Publisher's Note Springer Nature remains neutral with regard to jurisdictional claims in published maps and institutional affiliations.